Cellulose (2017) 24:1493–1509
DOI 10.1007/s10570-016-1178-5

ORIGINAL PAPER

Eco-friendly fabrication of antibacterial cotton fibers by the cooperative self-assembly of hyperbranched poly(amidoamine)- and hyperbranched poly(amine-ester)-functionalized silver nanoparticles

Sijun Xu · Feng Zhang · Lirong Yao · Chunhong Zhu · Hideaki Morikawa · Yuyue Chen

Received: 31 August 2016 / Accepted: 19 December 2016 / Published online: 2 January 2017

Abstract Wastewater has long been a highly important insurmountable problem in the textile industry. Since the rapid development of antimicrobial silver nanoparticle (AgNP)-coated textiles in the recent several decades, AgNP-containing wastewater produced in the finishing process has gradually posed a greater threat to the ecological environment than that by traditional organic dyes because of the former's strong antimicrobial ability. Herein, we designed an environmentally friendly, energy-efficient, bottom-up nanocoating strategy for cotton fibers through the cooperative self-assembly of heterogeneous AgNPs functionalized by amino-terminated hyperbranched poly(amidoamine) (HBPAA) and hydroxyl-terminated hyperbranched poly(amine-ester) (HBPAE), respectively. The HBPAA-functionalized AgNPs possessed a positive surface charge of +40.8 mV and dense amino end groups, whereas the HBPAE-functionalized AgNPs had a slightly negative surface charge (−15.8 mV) and abundant OH end groups. Therefore, given the intermolecular recognition and interactions between HBPAA and HBPAE, the heterostructured AgNPs selectively co-precipitated on the natural fiber surfaces. Our scanning electron microscopy (SEM), field emission SEM, and X-ray photoelectron spectroscopy studies confirmed that the heterostructured AgNPs were uniformly anchored on the surface of the cotton fibers, indicative of their excellent physical and prolonged chemical stability. The coated cotton fibers showed excellent antibacterial activity. At the extremely low Ag content of 3 mg/g, the coated cotton fibers showed satisfactory antibacterial effects with over 99% antimicrobial rates. The developed cooperative self-assembly strategy demonstrated a nearly complete AgNP uptake by natural fibers and the ability to precisely control silver content. As such, the cooperative self-assembly method promises a high potential for practical production.

Keywords Silver nanoparticles · Cotton · Cooperative self-assembly

S. Xu · L. Yao
School of Textile and Clothing, Nantong University, Nantong 226019, People's Republic of China

S. Xu · C. Zhu · H. Morikawa
Faculty of Textile Science and Technology, Shinshu University, 3-15-1 Tokida, Ueda, Nagano 386-8567, Japan

F. Zhang
Department of Textile Engineering, Shazhou Professional Institute of Technology, Zhangjiagang 215600, People's Republic of China

Y. Chen (✉)
College of Textile and Clothing Engineering, Soochow University, Suzhou 215021, People's Republic of China
e-mail: chenyy@suda.edu.cn

Introduction

Cotton fibers and fabrics are among the most popular and best-selling biomaterials worldwide for their wide application in clothes, home furnishings, and various textile-based industrial products, such as toys, home accessories, and medical gauzes and bandages (Bao and Li 2012). Such variety can be attributed to the materials' excellent mechanical and thermal properties, including excellent hygroscopicity and breathability, high strength and flexibility, and good thermal insulation. As a natural and abundant biomaterial, cotton is mainly composed of cellulose with polymerization degree ranging from 1×10^4 to 1×10^5. The supramolecular structure of cotton can be divided into three levels (Lee et al. 2000). Initially, dozens of cellulose macromolecules are combined to form a crystallized microfibril with a diameter of 6 nm through intermolecular interactions mainly dominated by hydrogen bonding. Several elementary fibrils are further assembled into fibrils of diameter range 10–25 nm. The fibrils further formed macrofibrils 0.1–1.5 μm in diameter and finally the cotton fiber.

Recently, scientists focused extensive research on the surface modification of natural fibers to improve or impart new physical and chemical fiber properties. One interesting strategy is to coat the natural fiber with nanomaterials and consequently convert the natural fiber into a multifunctional material. The resultant material is projected to not only integrate the advantages of both natural fiber and nanomaterial but also overcome their instinct drawbacks or even create new performances from their intrinsic properties (Hsu et al. 2015; Lu et al. 2015). Such functional natural fibers are helpful in transforming natural fibers into high-technology, high-added-value products with advanced functionalities (Eckhardt et al. 2013; Khan et al. 2016; Liu et al. 2013; Schoen et al. 2010; Zeng et al. 2014). One hotspot for research is the design and engineering of antimicrobial textiles by integrating antimicrobial nanomaterials into textile fiber.

Since ancient times, metallic silver has been known by mankind for its antimicrobial properties (Eckhardt et al. 2013). With the booming development of nanoscience and nanotechnology and an increased risk of bacterial resistance to existing organic antimicrobial agents, a new form of silver, that is, silver nanoparticle (AgNPs), has become a popular subject because of its superiority to bulk silver and organic antibiotics. Such advantage includes robustness and broad-spectrum antimicrobial activity, low bacterial resistance, and high biosafety (Rai et al. 2009). Although the exact antimicrobial mechanism remains under debate, researchers tend to believe that the antimicrobial ability of AgNPs mainly derives from the interaction of the Ag ions released from nanoparticle (NP) surfaces with important proteins and enzymes and the oxygen stress caused by peroxides such as O_2^- and OH^- formed on the AgNP surfaces (Levard et al. 2012). Owing to the excellent antimicrobial activity and unique antimicrobial mechanism, AgNPs have been widely used in food preservation, water disinfection, and medical devices (Yu et al. 2013). Nevertheless, recent studies proposed that AgNPs may pose a potential threat to the eco-environment. AgNP toxicity has been observed in unicellular aquatic flora and fauna, which are the basis of the biological chain (Levard et al. 2012). Therefore, reducing waste AgNPs is of great concern for their further development. In general, AgNPs can be discharged to the environment in every phase of manufacture and use of antibacterial products. To eliminate potential environment risk, recent research has been devoted for designing a green synthetic approach for AgNPs by carefully engineering their core–shell structure (Richter et al. 2015; Roopan et al. 2013). Studies also attempted to improve the combination between AgNPs and the fiber. However, few works were dedicated to the elimination of discharged AgNPs during the production process of antibacterial fibers or textiles. We point out that the waste AgNPs produced during the manufacture process may pose an even greater threat. The continuous emissions of substantial amounts of AgNP-containing wastewater in certain areas may not only quickly change the ecological structure because of their strong antimicrobial effects but may also adversely affect humanity through the bioaccumulation and concentration of the Ag element through the water food chain (Kaegi et al. 2013).

Traditional coating strategies of nanomaterials on biological fibers mainly depend on solution-based assembly technology, which mainly involves pad-dry-cure finishing, spraying, in situ deposition, and sol–gel coating (Huda et al. 2010). However, given the lack of sufficient compatibility to biological materials, the highly efficient AgNP uptake by biological fibers remains an insurmountable problem. In addition, given the amorphous surface nature of chemically

synthesized AgNPs, physically assembled AgNPs by in situ deposition and sol–gel coating are prone to oxidation and consequently accelerate the dissolution in water. Therefore, to successfully design and engineer an eco-friendly coating strategy for AgNPs on biological fibers, the AgNPs should possess three vital properties, namely, high chemical and water stability and high binding ability to biological molecules.

Molecule-induced NP self-assembly on the biomolecule surface is described as the spontaneous spatial arrangement of NPs functionalized by functional polymers that can recognize biomolecular targets (Grzelczak et al. 2010). This spatial arrangement is driven by electrostatic attraction, hydrogen bonding, and host–guest interactions. As such, the self-assembly may provide an alternative eco-friendly method for generating NP coatings that can overcome the above-mentioned shortcomings (Kuzyk et al. 2012; Li et al. 2015; Nykypanchuk et al. 2008; Rogers et al. 2016; Zhang et al. 2013). The advantages of such bottom-up strategies lie in the simplicity and high efficiency of the preparation process. In our previous study, AgNPs functionalized by amino-terminated hyperbranched poly(amidoamine) (HBPAA) were successfully designed and found capable of being completely adsorbed by carboxyl-rich alginate fibers and hydroxyl-containing silk fibers depending on the strong molecular interactions between the capping molecule and the biomolecule on the fiber surfaces (Xu et al. 2016a, 2015). However, this strategy achieves lower efficiency for cotton compared with the above-mentioned biological fibers because of the relatively inert hydroxyl groups on the cotton surface. In fact, the surface AgNP charges adversely influence AgNP properties in the following manners: (1) the charges improve AgNP water stability and provide electrostatic attractions toward the oppositely charged fiber surface or (2) inhibit their attachment on the oppositely charged fiber surface because of the charge repulsion among NPs. To overcome this barrier, we developed an NP cooperative self-assembly technology by designing two distinct AgNPs with the NP surfaces functionalized with amino-terminated HBPAA and hyperbranched poly(amine-ester)s (HBPAE) capable of mutual recognition and combination to overcome the charge steric hindrance. Such charge steric hindrance was surmounted by converting the electrostatic repulsion among NPs to electrostatic attractions. Particularly, the AgNP coating was constructed by the alternate self-assembly of positively charged HBPAA/AgNPs and negatively charged hydroxyl-terminated HBPAE-functionalized AgNPs (HBPAE/AgNPs) on the cotton fiber surfaces. HBPAA and HBPAE were selected as capping agents because of their similarly unique advantages of 3D spatial structure, amphipathicity, and dense functional end groups. As such, the agents afforded the AgNPs with good protection from agglomeration and corrosion. Meanwhile, the agents also enabled mutual recognition and combination because of their opposite charges and ability to form hydrogen bonds through amino–hydroxyl interactions.

In this study, we designed a highly efficient and eco-friendly self-assembly approach to fabricate heterostructured AgNP-coated cotton fibers by NP cooperative self-assembly technology. In such system, cotton fibers served as the substrate, whereas the positively charged amino-dominated HBPAA-functionalized AgNPs (HBPAA/AgNPs) and negatively charged hydroxyl-dominated HBPAE/AgNPs served as the cooperative building blocks. The surface modification of HBPAA and HBPAE aimed to enhance the agents' binding capacity to hydroxyl-dominated cotton cellulose, impart high water and chemical stability to the AgNPs, and generate heterogeneous NPs that can mutually recognize and combine depending on the collective supramolecular interactions of long-range electrostatic attractions and short-range hydrogen-bonding interactions. AgNP coating was formed by the circular introduction of HBPAA/AgNPs and HBPAE/AgNPs to the cotton surface through a simple cyclic impregnation method. To realize the concept of environmental protection, HBPAA/AgNPs and HBPAE/AgNPs were completely adsorbed on the cotton surface by appropriately adjusting experimental conditions. The physical–chemical properties of the coated cotton were evaluated by Fourier transform infrared spectroscopy (FTIR), scanning electron microscopy (SEM), X-ray photoelectron spectroscopy (XPS), X-ray diffraction (XRD).

Experimental section

Materials

Cotton fibers were purchased from Zhangjiagang Nellnano Nanotechnology Co., Ltd. (China). HBPAE

and HBPAA were synthesized by previously reported methods (Xu et al. 2016a). Silver nitrate ($AgNO_3$), ethanol (99.5%), sodium borohydride, and nitric acid (HNO_3, ~70%) were purchased from Wako Pure Chemical Industries, Ltd. (Japan). *Escherichia coli* (ATCC8099) and *Staphylococcus aureus* (ATCC 6538) were obtained from the College of Life Sciences, Soochow University (China). Nutrient broth and nutrient agar were purchased from Wako Pure Chemical Industries, Ltd. (Japan).

Synthesis of HBPAA/AgNPs and HBAPE/AgNPs

Prior to the synthesis of functional AgNPs, HBPAE and HBPAA were dialyzed against deionized water using SnakeSkin® dialysis tubings (Thermo Scientific, molecular weight cut-off: 3500 Da) for 24 h to remove any oligomers.

HBPAA/AgNPs were synthesized as described by our previously reported method. Specifically, HBPAA/AgNPs were fabricated by dissolving 2 g HBPAA in 45 mL deionized water and adding HBPAA solution to 5 mL of 7.8 g/L silver nitrate aqueous solution at 35 °C using a well-described procedure. The reaction mixture was slowly heated to 90 °C and kept stirring at 90 °C for 3 h. The resulting product was maintained in the refrigerator.

HBPAE/AgNPs: Briefly, 5 mL of 7.8 g/L silver nitrate aqueous solution was mixed with 45 mL of 12 g/L HBPAE solution under magnetic stirring at 30 °C. This step was followed by the addition of 5 mL of 1 g/L of sodium borohydride to the $AgNO_3$/HBPAE mixture. The as-prepared AgNP samples were then stored in the refrigerator.

Cooperative self-assembly of HBPAA/AgNPs and HBPAE/AgNPs on cotton fibers

The heterostructured AgNP coating was constructed by alternately coating HBPAA- and HBAPE-functionalized AgNPs on cotton fibers with final high-temperature curing. Primarily, their concentration ratio was set as 1:1 to ensure that the HBPAA/AgNPs and HBPAE/AgNPs could be completely adsorbed by cotton through their cooperative adsorption. The bottleneck of the self-assembly was the initial adsorption of HBPAA/AgNPs by cotton fibers because their binding ability was much weaker than between HBPAA/AgNPs and HBPAE/AgNPs. Therefore, to guarantee the complete uptake of HBPAA/AgNPs, the optimal conditions should be first determined.

The effect of Ag concentration and incubation temperature on the adsorption of single HBPAA/AgNPs by cotton fibers was investigated to find their optimal conditions for the complete uptake of HBPAA/AgNPs by cotton fibers. Specifically, 1 g of fiber samples was completely infiltrated by pre-impregnation in deionized water for 10 min. The wet cotton fibers were then transformed onto 100 mL of solution of HBPAA/AgNPs with concentrations ranging from 10 to 100 mg/L. The mixture was then stirred for 120 min at 35–95 °C. The HBPAA/AgNP-coated cotton fibers were removed and washed with deionized water three times. The remaining concentration of HBPAA/AgNPs in the solution was measured by inductively coupled plasma atomic emission spectrometry (ICP–AES). The Ag content of the treated cotton fibers was then calculated by the following formula:

$$C_{ag} = \frac{C_o - C_t}{10} \quad (1)$$

where C_{ag}, Co, and C_t are the Ag content of coated cotton fibers, initial concentration of HBPAA/AgNPs, and the concentration of HBPAA/AgNPs in the residual solution, respectively.

The HBPAA/AgNP-coated cotton fibers prepared under optimal conditions were circularly incubated with 100 mL of solutions of HBPAE/AgNPs and HBPAA/AgNPs with the above-determined concentration and temperature and incubation time of 0.5 h under stirring. After several times of treatment (including initial treatment by single HBPAA/AgNPs), a dense and controllable nanocoating was formed on the cotton surface. Finally, the as-prepared fiber samples were cleaned by tap water several times, cured in an oven at 120 °C for 20 min, and stored in a seal sample bag.

Sample characterization

AgNP morphology was studied by transmission electron microscopy (TEM; JEM-2100F, JEOL, Japan). The hydrodynamic size and surface AgNP charge in the aqueous solution were evaluated using the Nano ZS90 Zetasizer (Malvern, UK). The UV–vis spectra at 300–700 nm were obtained using a UV-2700 spectrophotometer (Shimadzu, Japan). The Ag content was

measured in acidified solutions by ICP–AES (Vista MPX; Varian, USA).

The morphology and size of AgNPs on the fiber were characterized and analyzed by scanning electron microscopy SEM (Hitachi S-3000 N, Hitachi, Japan) and field emission SEM (FESEM; Hitachi S-5000, Hitachi, Japan). The FTIR was collected on a Perkin Elmer Spectrum 100 FTIR spectrometer (Perkin Elmer, USA), which converted fiber samples into powder using the KBr pellet infrared spectrometer test under a scan number of 32 and resolution of 4 cm^{-1}. The chemical states and crystal structures of samples were analysed by XPS (AXIS Ultra DLD; Krotos, Japan) and XRD (D8 ADVANCE, Bruker, Germany). Thermogravimetric analysis of samples was performed on a thermogravimetric analyzer in nitrogen atmosphere (TG 209 F3 Tarsus, Germany Netzsch Instruments, Inc.) within the temperature range of 40–650 °C at a scanning rate of 10 °C/min. The mechanical analysis was conducted using XQ-1A fiber tensile tester (Shanghai New Fiber Instrument Co., Ltd., China). The fineness of the fibers was measured by XD-1 vibration fiber fineness tester (Shanghai New Fiber Instrument Co., Ltd., China). For each sample, 20 specimens were tested. The fineness of the fibers was measured in terms of dtex, which is the weight of the fibers in grams per 10,000.

Evaluation of the antibacterial activity of the natural fibers

The antimicrobial activity of the cotton fibers was measured against *E. coli* and *S. aureus* using a shake-flask method (GB/T 20944.3-2008 [China]). Briefly, the test and control cotton fibers (0.75 g) were immersed into a flask containing 70 mL 0.3 mM PBS (monopotassium phosphate, ~pH 7.2) culture solution with cell concentration of 1×10^5–4×10^5 colony forming units (cfu)/mL in triplicates. Subsequently, the flasks were subjected to incubation on a rotary shaker at 24 °C for 18 h. The colonies formed after incubation were counted by spread-plating serial dilutions on an agar plate at 24 h. The percentage reduction (C, %) was determined using the following formula:

$$C = \frac{B - A}{B} \quad (2)$$

where C and A are the bacterial colonies of the control and treated cotton fibers, respectively.

Results and discussion

Characterization of HBAPA/AgNPs and HBPAE/AgNPs

Given the weak interactions between cotton and metallic AgNPs which is mainly dominated by van der Waals forces, the poor compatibility of metallic AgNPs with biological fibers usually leads to low assembly efficiency, weak adhesive strength, and high environmental risks. Therefore, recent research focus has shifted to promoting their binding affinity by various strategies, such as modifying or grafting the fiber surface with cationic polyelectrolytes or cationic groups. Collectively, these strategies aim to convert weak van der Waals forces to robust long/short-range intermolecular forces, such as electrostatic, hydrophobic, and hydrogen-bonding forces, with final improvement of their combination. However, this approach suffers from certain deterioration of mechanics and gloss of fibers. Recently, we adopted the opposite supramolecular self-assembly strategy: capping the AgNP surface with amino-terminated HBPAA to guide and immobilize NPs to the fiber surface by intermolecular electrostatic and hydrogen-bonding interactions while avoiding potential fiber damages (Xu et al. 2016b). However, such approach remains sensitive to the surface chemical properties of biological fibers.

To remedy this limitation, we further developed a supramolecular cooperative self-assembly by alternate assembly of mutual recognized donor/acceptor molecule-capped AgNPs on the fiber surface mediated by supramolecular interactions among HBPAA, HBPAE, and cotton cellulose. The detailed self-assembly mechanism and procedure is illustrated in Fig. 1. We first synthesized two heterostructured AgNPs separately functionalized with amino-terminated HBPAA and hydroxyl-terminated HBPAE. HBPAA and HBPAE were used as capping agents because these substances possess similar molecular features, including amphiphathicity, 3D quasi-spherical structure, and abundant functional end groups suitable for protecting and stabilizing AgNPs. Meanwhile, these agents endow two heterostructured AgNPs with a special ability of mutual recognition and combination derived from the supramolecular electrostatic attraction and multiple hydrogen-bonding interactions between HBPAA and HBAPE. The self-assembly is initially

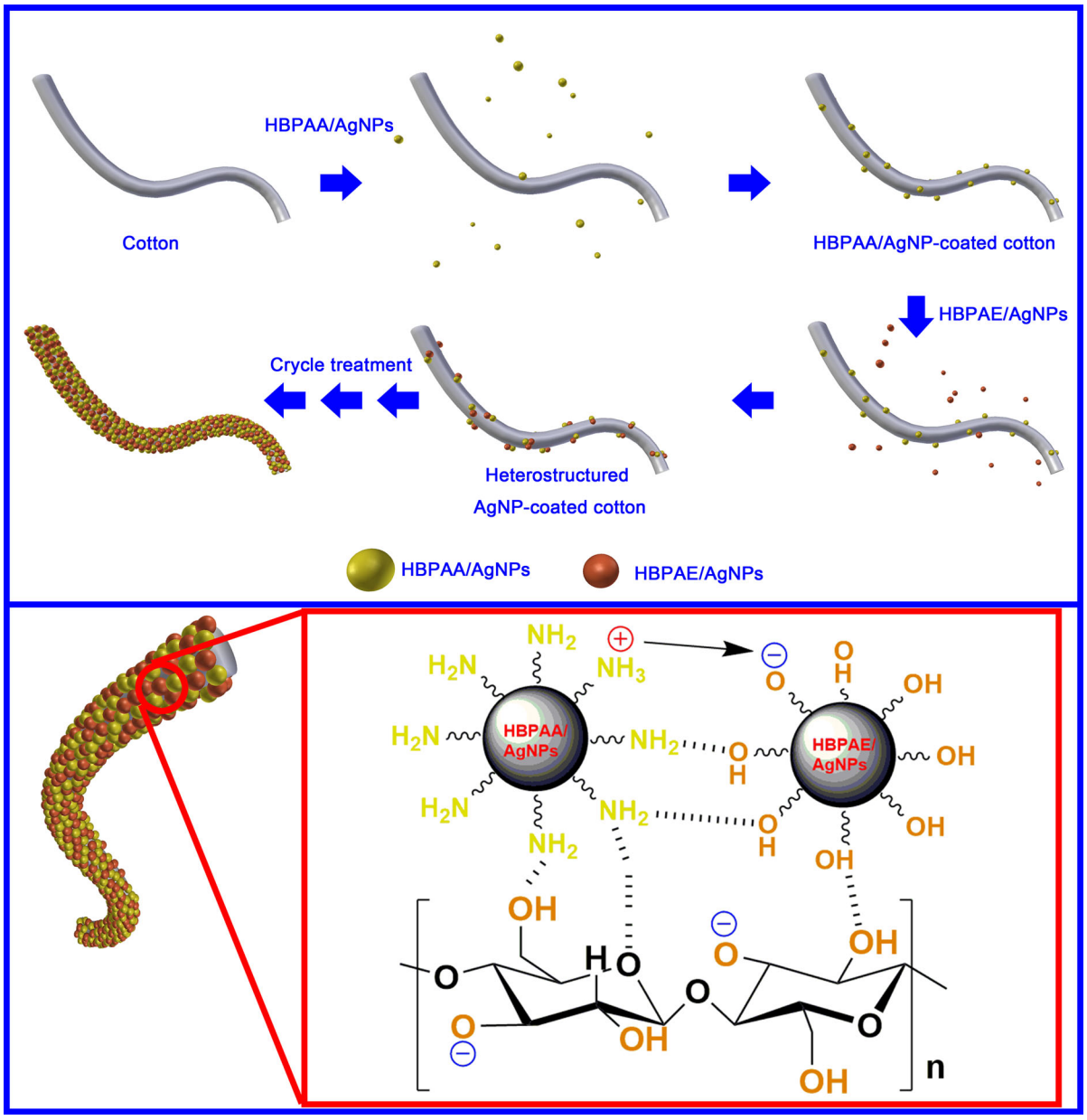

Fig. 1 Schematic representation of cooperative self-assembly of HBPAA/AgNPs and HBPAE/AgNPs on cotton fiber surfaces

triggered by electrostatic and hydrogen-bonding interactions between amino-functionalized HBPAA/AgNPs and hydroxyl-dominated cotton cellulose because HBPAA anchored to AgNP surfaces possesses much higher binding ability to cotton cellulose than does hydroxyl-terminated HBPAE depending on their dense functional amino groups and polycationic features (Fig. 1). Nevertheless, given the relative chemical inertness of semicrystalline cotton cellulose, such intermolecular interactions are insufficient to overcome the combined obstacles of thermal energy and electrostatic repulsion among HBPAA/AgNPs, which is necessary to guide the massive HBPAA/AgNPs onto the cotton surface. Nonetheless, this disadvantage could be reversed by the alternate introduction of HBPAA/AgNPs and HBPAE/AgNPs onto the cotton surface for transforming electrostatic repulsion into electrostatic attraction (Fig. 1). By

circular incubation with oppositely charged HBPAE/AgNPs and HBPAA/AgNPs, the attached heterostructured AgNPs shift turns to serve as trapping agents for oppositely charged AgNPs and further form multi-hydrogen bonding interactions, resulting in co-attachment of heterostructured AgNPs on cotton surfaces. Theoretically, a dense AgNP coating with controllable Ag content and environmentally friendly self-assembly procedure can be achieved by multi-cycle incubation of two reversed AgNPs and by ensuring the complete adsorption of AgNPs in each step through the careful design of experimental conditions.

In summary, the self-assembly mechanism of heterostructured AgNPs on cotton fibers was mainly dependent on electrostatic and hydrogen bonding interactions. Given that such intermolecular interactions were much stronger than the van der Waals forces, as-prepared AgNP coatings were expected to show higher firmness than traditional methods. Nevertheless, there interactions were easily broken by detergent surfactants; therefore, washing fastness would be lower than that combined by chemical interactions. Considering that as-prepared cotton was designed to manufacture disposable medical dressing, excellent washing fastness was unnecessary.

The synthetic methods of HBPAA/AgNPs and HBPAE/AgNPs were slightly dissimilar. HBPAA/AgNPs were synthesized by the hydrothermal reduction of $AgNO_3$, with HBPAA acting as the reducing and capping agent because of its reductive amino groups. By contrast, HBPAE/AgNPs were prepared by reducing an aqueous solution of $AgNO_3$ using $NaBH_4$ at ambient temperature with HBPAE only serving as the capping agent because of HBPAE's weak reducibility. Figure 2a shows the TEM image of monodispersed HBPAA/AgNPs with about 14.9 nm average diameter, in line with the hydrodynamic size measured by DLS (inset of Fig. 2a). The observed large-scale HBPAA/AgNPs exhibited uniform sizes and a regular spherical structure, which were probably contributed by the relatively low reaction rate and rigorous space restriction of HBPAA. In comparison, the average hydrodynamic size of HBPAE/AgNPs possesses a much smaller hydrodynamic size of around 4.4 nm (Fig. 2b inset), and a slightly wide size distribution was observed from the TEM images (Fig. 2b). Moreover, the amino-terminated HBPAA and hydroxyl-terminated HBPAE not only impart the nano-size and good water stability to AgNPs but also opposite surface charges and complementary surface functional groups capable of mutual recognition and combination. The HBPAA/AgNPs possess a positive surface potential (+40.8 mV) derived from the numerous cationic amino groups in HBPAA (Fig. 2e). Conversely, HBPAE/AgNPs exhibited a slightly negative charge (−15.8 mV) attributed to the weakly acidic nature of HBPAE (Fig. 2f). The binding of HBPAA and HBPAE has been proven in our previous studies. The good capping effects of HBPAA and HBPAE on AgNPs were probably due to their 3D cavity structure, abundant functional end groups, and their amphipathic characteristic.

Cooperative self-assembly of HBPAA/AgNPs and HBPAE/AgNPs on cotton fibers

To eliminate potential environmental risks during the treatment, a fundamental principle is that two heterostructured AgNPs should adsorb onto cotton fibers completely in each step. Thus, the concentration ratio between HBPAA/AgNPs and HBPAE/AgNPs was set as 1:1 to ensure their synergistically complete adsorption by cotton fibers. In our experiment, coating cotton fibers with heterostructured AgNPs was performed by cycle incubation of cotton fibers with colloidal solutions of HBPAA/AgNPs and HBPAE/AgNPs. Specifically, cotton fibers are first incubated with a colloidal solution of HBPAA/AgNPs for 2 h. HBPAA/AgNPs were used as the starting coating solution because of their much stronger binding affinity to cotton cellulose than that of HBPAE/AgNPs attributed to the former's opposite positive charges and high number of amino surface groups.

HBPAA/AgNPs exhibited a relatively weak bind ability. Hence, the material's adsorptive ability on cotton should be investigated to determine the optimum conditions for complete transfer of HBPAA/AgNPs from colloidal solution to cotton surfaces. HBPAA/AgNPs demonstrated temperature-dependent adsorption, i.e. the adsorption capacity of HBPAA/AgNPs increased with increasing incubation temperature (Fig. 3a). By setting the incubation temperature to 85 °C, we further investigated the Ag-concentration-dependent adsorption efficiency. Cotton fibers showed a nearly 100% uptake of HBPAA/AgNPs when the HBPAA/AgNP concentration is below 50 mg/L (Fig. 3b). Conversely, with the further concentration rise from 50 to 100 mg/L, the adsorption

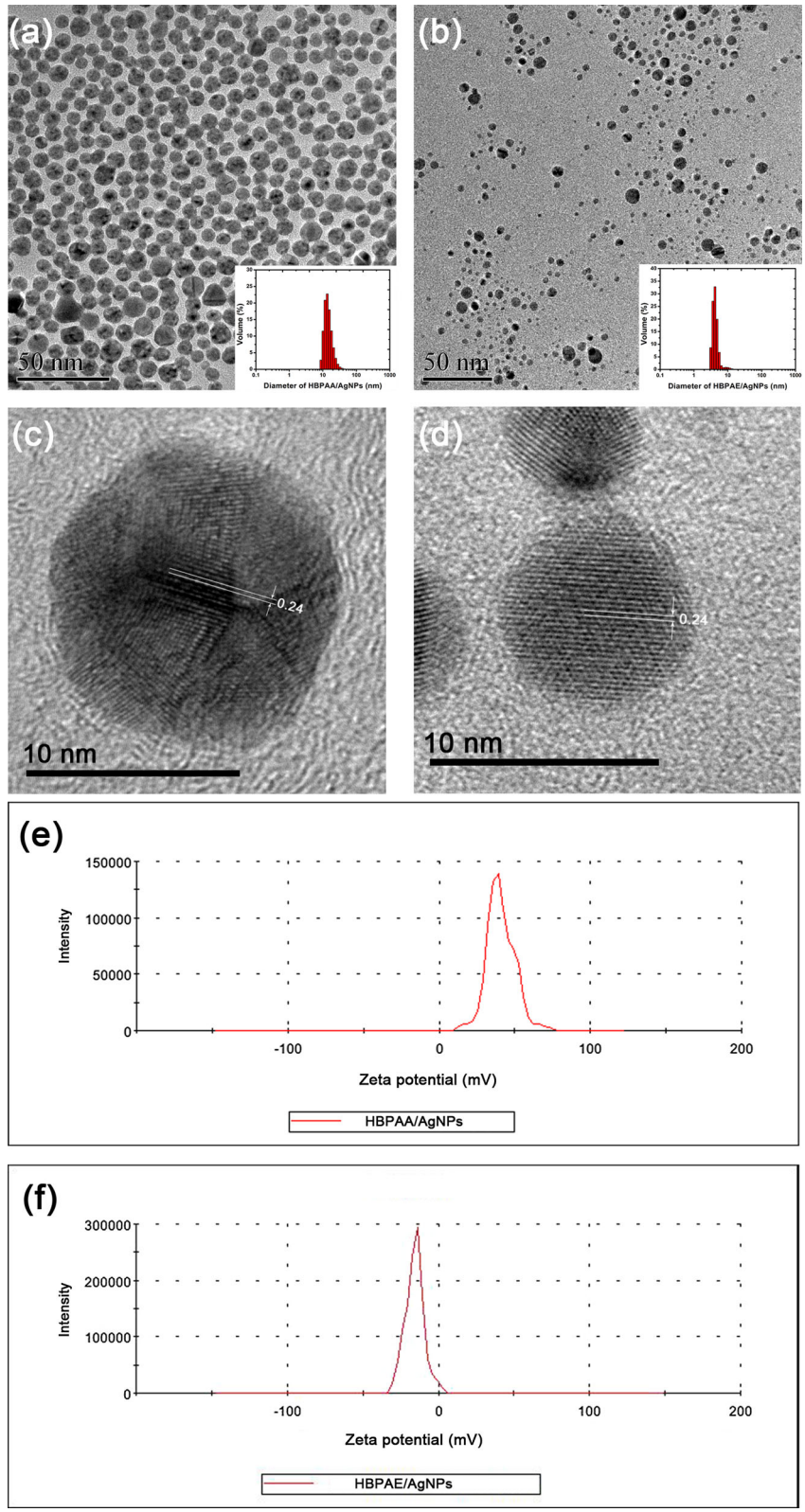

Fig. 2 TEM and high-resolution TEM images of **a**, **c** HBPAA/AgNPs and **b**, **d** HBPAE/AgNPs. Zeta potential of **e** HBPAA/AgNPs and **f** HBPAE/AgNPs. In situ size distribution measured by DLS of HBPAA/AgNPs and HBPAE/AgNPs are shown in the inset of Figs. 1a and 1b, respectively

efficiency of HBPAA/AgNPs by cotton continuously decreased from nearly 100–29%. In summary, the experimental conditions for complete adsorption were the concentration range 0–50 mg/L and the incubation temperature of 85 °C.

By coating the cotton surface with HBPAA/AgNPs, the subsequent cooperative self-assembly between HBPAA/AgNPs and HBPAE/AgNPs was highly simplified because of their ultra-strong intermolecular interactions. HBPAA/AgNP-coated cotton fibers prepared by the aforementioned optimum experimental conditions were circularly transferred into colloidal solutions of HBPAE/AgNPs and HBPAA/AgNPs with the same concentration (as determined above) under continuous stirring. In this stage, HBPAA/AgNPs and HBPAE/AgNPs alternately served as trapping agents for opposite AgNPs. Therefore, the adsorption rate

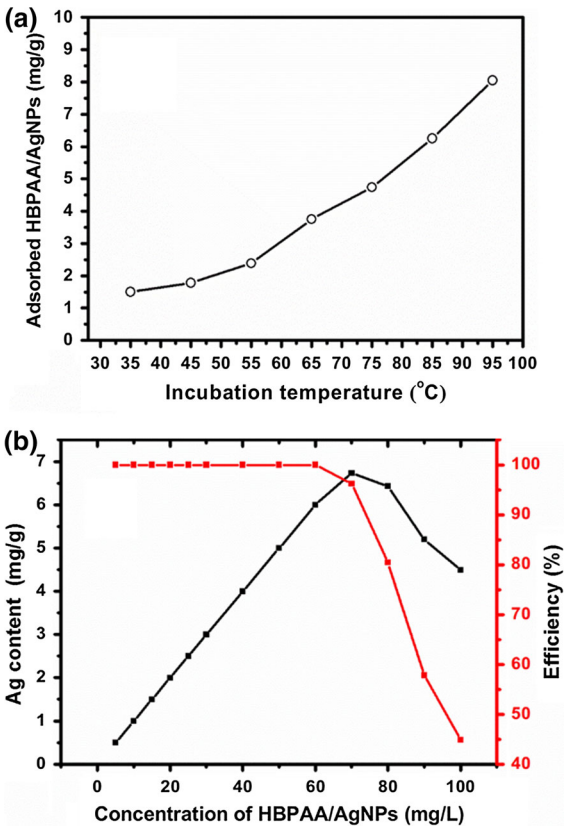

Fig. 3 Adsorption of HBPAA/AgNP by cotton as a function of **a** incubation temperature (HBPAA/AgNP concentration: 100 mg/L; incubation time: 2 h). The HBPAA/AgNPs adsorbed by cotton as a function of **b** HBPAA/AgNP concentration in the colloidal solution (incubation temperature: 85 °C; incubation time: 2 h)

was much faster than that between HBPAA/AgNPs and cotton. Our study showed that the complete adsorption between HBPAA/AgNPs and HBPAE/AgNPs was achieved within 30 min. This occurrence can be attributed to good supramolecular recognition and combination between HBPAA and HBPAE.

Given that AgNPs were completely assembled onto cotton surface, the Ag content ($C_{cot,}$, mg/g) of coated cotton fibers can be calculated by the following formula:

$$C_{cot} = \frac{\mathrm{n} \times C_{sol}}{10} \tag{3}$$

where C_{sol} and n are the concentrations of AgNP solution and treatment times, respectively. The concentrations of HBPAA/AgNPs and HBPAE/AgNPs were equal.

Figure 4 demonstrates the specific self-assembly process for 15 mg/g of heterostructured AgNP-coated cotton fibers. The time-lapse color changes of solutions of HBPAA/AgNPs and HBAPE/AgNPs and cotton fibers represented the spatial transfer of AgNPs from aqueous phase to solid cotton surfaces. During incubation with HBPAA/AgNPs, the white color of cotton fibers slowly transformed to luminous yellow after 2 h contact time at 85 °C. Such effect was accompanied by the color fading of the HBPAE/AgNPs solution from golden yellow to colorless, indicative of the spatial transfer of yellow-colored AgNPs from the aqueous phase to the solid cotton surfaces. Conversely, the characteristic yellow color of HBPAE/AgNPs quickly disappeared within 30 min after incubation the HBPAA/AgNP-coated cotton fibers in a solution of HBPAE/AgNPs. This result suggests the strong combination capacity between HBPAE and HBPAA. After three times of cycle treatment, the resultant cotton fibers finally attained a dark yellow color with Ag content of nearly 15 mg/g.

FTIR analysis

HBPAA and HBPAE capping of the AgNP surface plays a vital role in self-assembly because the agents impart the surfaces of heterostructured AgNPs with functional 3D polymer shells that possess opposite surface charges and abundant electron-donating or electron-accepting groups, respectively. These groups not only protect and stabilize the AgNPs in colloidal solution but also endow the AgNPs with certain

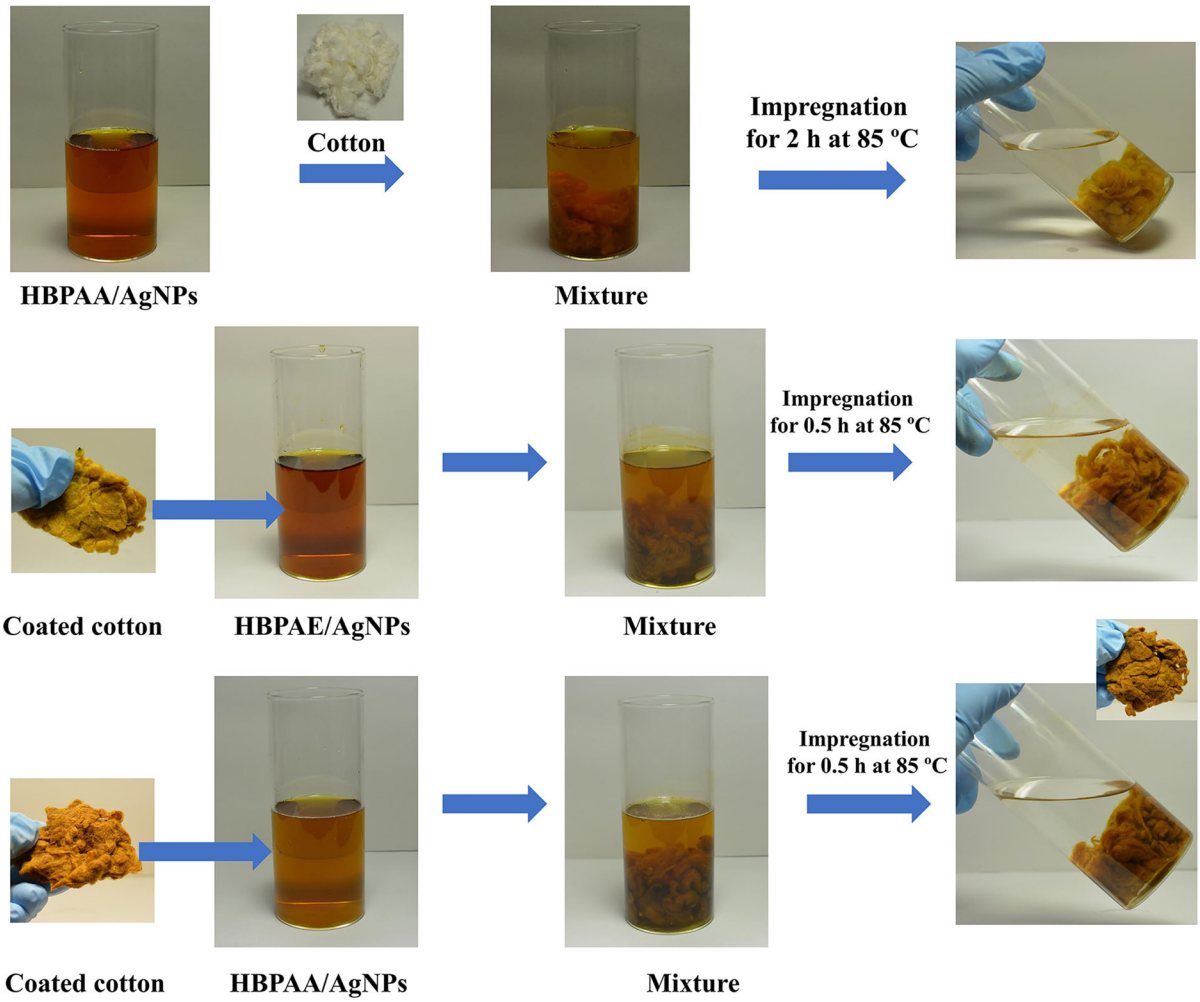

Fig. 4 Preparation process for 15 mg/g of heterostructured AgNP-coated cotton fibers. Cotton fibers were incubated alternately in 50 mg/L solutions of HBPAA/AgNPs and HBAPE/AgNPs

molecular recognition and combination ability. Therefore, NP transfer onto the cotton surface would accompany the chemical combination of HBPAA, HBAPE, and cotton cellulose. FTIR spectroscopy is a useful tool for representing the chemical composition, spatial configuration, and functional groups of organic materials. As such, FTIR can be utilized to confirm the existence of HBPAA and HBPAE and analyze the potential physiochemical influence of HBPAE and HBPAA on cotton. The FTIR spectrum of the pristine cotton fibers showed the typical characteristic peaks of cotton cellulose (Fig. 5b) (Abidi et al. 2008). The broad band from 3200 to 3500 cm^{-1} could be assigned to O–H stretching (intermolecular hydrogen bonds). The vibrations located at around 2918 and 2850 cm^{-1} were attributed to CH_2 asymmetric stretching, which originates from the cellulose in the cell walls of cotton and wax substances attached on the cotton fiber surfaces. The band centered at around 1640 cm^{-1} corresponded to the deformation vibration of absorbed water molecules through hydrogen bonding in the amorphous regions of the cellulose macromolecules. The bands of 1250–800 cm^{-1} represented the fingerprint of cotton cellulose, which could be assigned to the vibrations of the COH in-plane bending, antisymmetric bridge $C_{(1)}$–O–$C_{(4)}$ stretching, and C–O stretching. Notably, the vibrations located at 1161 and 896 cm^{-1} were attributed to the β-D-glucosidic bond, and their position and intensity were associated with the molecular weight of cotton cellulose. After

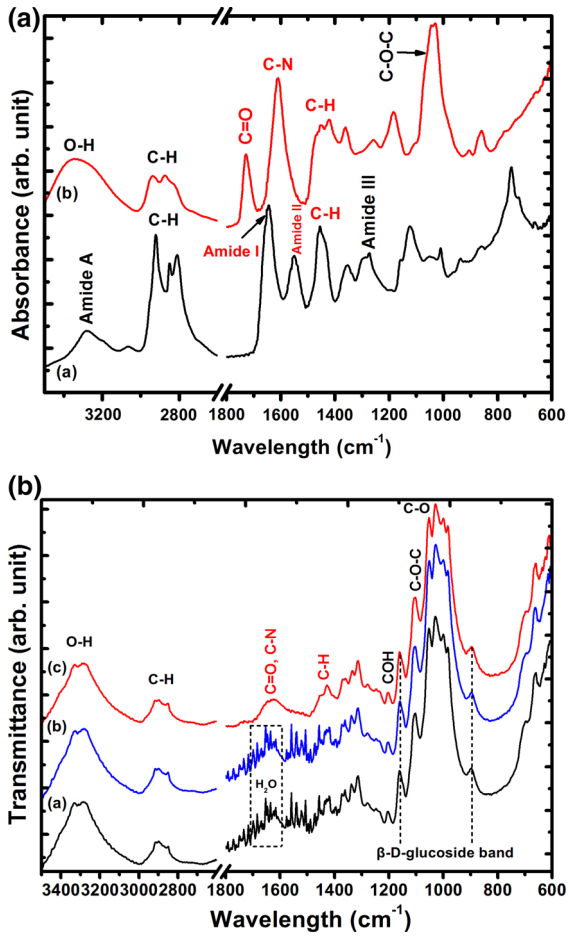

Fig. 5 **a** FTIR spectra of HBPAA (*black*) and HBPAE (*red*). **b** FTIR spectra of pristine cotton fibers (*black*), 3 mg/g (*blue*), and 15 mg/g (*red*) of heterostructured AgNP-coated cotton fibers. (Color figure online)

introducing various densities of heterostructured AgNP coatings to the cotton fibers, the main chemical bonds and related intensity of cotton cellulose, including O–H stretching, asymmetric C–H stretching, COH in-plane bending, C–O–C stretching, and C–O stretching, remained unchanged. This result implied the absence of major molecular structural change and secondary conformation during the cooperative self-assembly process.

The absorption bands and the intensity of combined water at 1650 cm^{-1} and CH_2 symmetric deformation at around 1429 cm^{-1} indirectly represent the proportion of amorphous and crystalline cellulose (Abidi et al. 2008). In the case of 3 mg/g of heterostructured AgNP-coated cotton fibers, these absorption bands showed almost the same intensity as that of the pristine cotton fibers, suggesting that the cooperative assembly process did not affect the crystal structure of cotton. Conversely, when Ag content increased to 15 mg/g, obvious changes in vibrations from 1750 to 1350 cm^{-1} were observed. The characteristic adsorption band of combined water around 1650 cm^{-1} was covered completely by absorption bands of amide I, amide II, and C–H vibrations in HBPAA and C=O, C–N, and C–H vibrations in HBPAE. This result suggests that HBPAE and HBPAA were anchored to the cotton, and their content were positively correlated to Ag content. The finding also implies that the cooperative self-assembly of the AgNPs achieved an important association with their functional capping molecules.

Morphological characterizations of functional cotton fibers

The morphologies and distribution states of AgNPs assembled on the cotton fiber surface significantly affect the function of the final nano-coating as observed by FESEM and SEM. The pristine cotton fibers exhibited unique morphological characteristics, including nature-formed convolution and parallel-arranged macrofibrils with a certain degree of orientation (Fig. 6a–c). After coating with HBPAA/AgNPs and HBPAE/AgNPs, an obvious distinction presented between the uncoated and AgNP-coated cotton fibers. Numerous monodispersed AgNPs and few AgNP clusters were uniformly scattered on the cotton surface when the Ag content was only 3 mg/g. Unlike monodispersed AgNPs on a fiber surface, the Ag cluster formation was attributed to the chemical interactions between HBPAA and HBPAE (Fig. 6e, f). Even so, the diameter of the constituent AgNPs in nanoclusters remained unchanged relative to the determined sizes of the HBPAA/AgNPs and HBPAE/AgNPs as observed under FESEM when the NPs transferred from water to the solid cotton surface. Hence, no crystallization growth of AgNPs occurred during the self-assembly process (Fig. 6f), indicating the assembled AgNPs inherited their intrinsic nanoproperties after the spatial transformation. By further increasing the concentration of the heterostructured AgNPs, we observed the coverage density of the AgNPs on the cotton surface to proportionally increase as

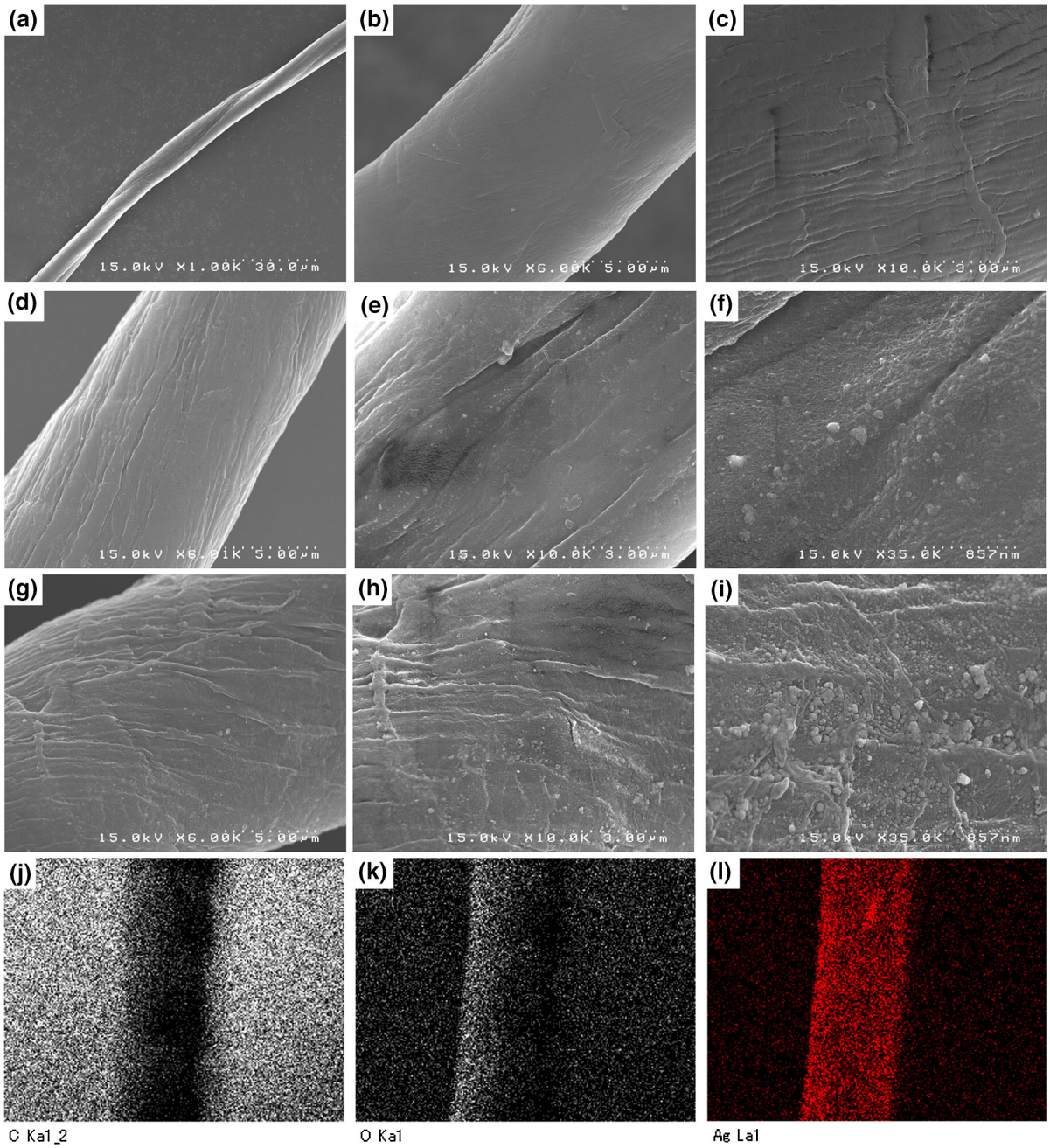

Fig. 6 FESEM images of **a**–**c** pure cotton, **d**–**f** 3 mg/g, and **g**–**i** 15 mg/g of heterostructured AgNP-coated cotton fibers. **j**–**l** Corresponding EDS element mapping images showing the distribution of C, O, and Ag elements obtained from SEM (Ag content: 15 mg/g)

expected. Although the monodispersed AgNPs remained as the dominant distribution mode compared with that under low AgNP content, the proportion of the heterostructured AgNP clusters was slightly enlarged (Fig. 6i). Notably, such coatings remained well distributed, suggesting that the heterostructured AgNPs tended to attach interfaces between the cotton and AgNPs rather than self-stack during the self-assembly

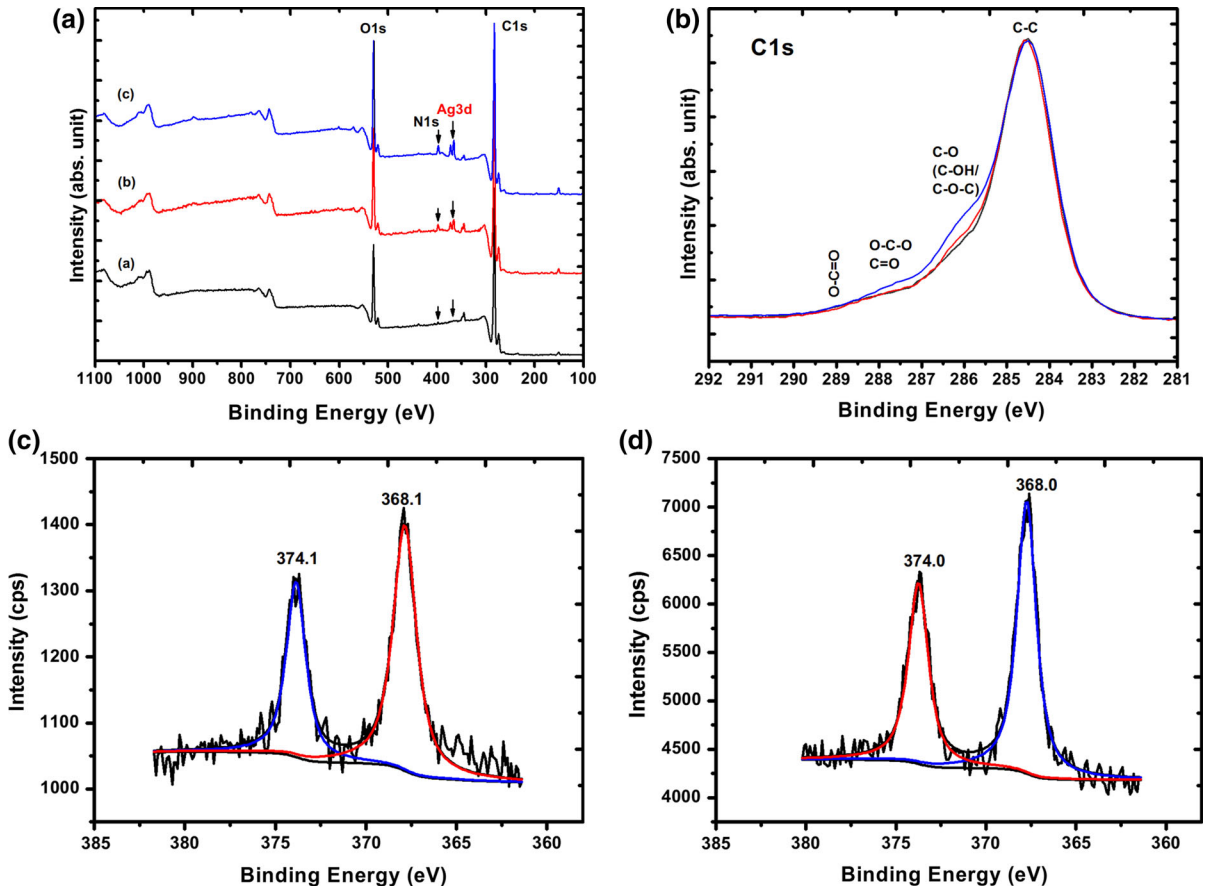

Fig. 7 **a** Wide-scan and **b** C1 s XPS spectra of pure cotton fibers (*black*) and 3 (*red*) and 15 mg/g (*blue*) of heterostructured AgNP-coated cotton fibers and **c**, **d** Ag3d XPS spectra of 3 and 15 mg/g of heterostructured AgNP-coated cotton fibers. (Color figure online)

process. This effect was probably caused by the combined intermolecular forces among the HBPAA/AgNPs, HBPAE/AgNPs, and cotton cellulose, making AgNPs preferentially anchor to the negatively charged cotton surface. The chemical characteristics of the nanocoating were further confirmed by the energy dispersive spectroscopy (EDS) mapping analysis of elements C, O, and Ag. Additional Ag element was found in the heterostructured AgNP-coated cotton fibers compared with the pristine cotton fibers (Fig. 6j–l), which may be ascribed to the attachment of metallic AgNPs to the cotton fibers. Notably, Ag distributed evenly across the cotton fiber surfaces, which was in good agreement with the FESEM measurements. This effect was mainly attributed to the ordered self-assembly of the heterostructured AgNPs on the cotton fiber surfaces.

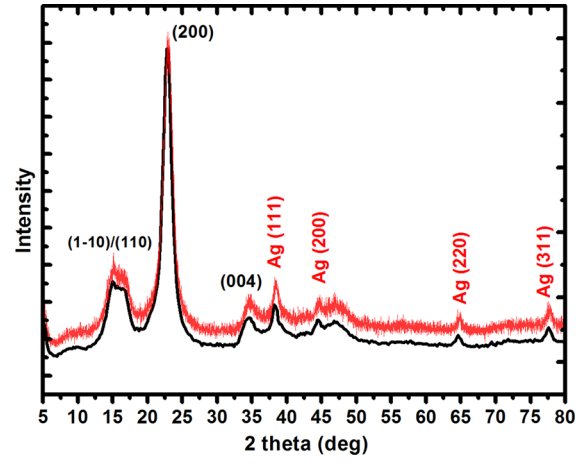

Fig. 8 XRD of the freshly prepared (*black*) heterostructured AgNP-coated cotton fibers (15 mg/g) and (*red*) stored for 1 month. (Color figure online)

XPS and XRD analysis

Metallic NPs are prone to corrosion when transferred from water to an oxygen (O_2)-rich air environment. Therefore, the capping of 3D-structured HBPAA and HBPAE serves another important purpose, i.e. the isolation of the NPs from O_2, with final improvement of the NPs' chemical stability. To verify the protective ability of the capping molecules, we conducted XPS to analyze the element valence states of the coated cotton fibers. Figure 7a shows the wide-scan XPS spectra of the pure cotton fibers and 3 and 15 mg/g of the heterostructured AgNP-coated cotton fibers. The pure cotton fibers showed only C1s and O1s peaks, whereas the coated cotton fibers presented an N1 s peak at around 400 eV and Ag3d peaks at around 374 and 368 eV, indicative of the attachment of the heterostructured AgNPs. The intensities of the N and Ag elements increased synchronously with increasing Ag content, suggesting their close integration. Moreover, the attachment of HBPAA and HBPAE could be further verified by analyzing the C1 s XPS spectra of cotton and the 3 and 15 mg/g samples of heterostructured AgNPs (Fig. 7b). The C1s peaks of the cotton fibers could be classified into four categories as follows: C–C (284.5 eV), C–O (286.4 eV), C=O (287.8 eV), and O–C=O (289.0 eV) (Peng et al. 2009). These peaks were attributed to cellulose and impurities, such as long-chain fatty acids. Notably, with rising Ag content of the coated cotton fibers, the intensities of the C–O and C=O peaks augmented, attributing to the increased content of HBPAA and HBPAE. The Ag3d deconvolution analysis (Fig. 7c, d) demonstrate that the heterostructured AgNPs maintained their metallic character when the AgNPs were transferred from water to the organic cotton surface.

To further examine the chemical stability, 15 mg/g of heterostructured AgNP-coated cotton fibers were stored in air for 1 month and then re-assessed by XRD. The expected (1–10)/(110), (200) and (004) cellulose I peaks (French 2014) were unchanged (Fig. 8). Also, the diffraction peaks at 38.1°, 44.2°, 64.4°, and 77.4° remained unchanged after 1 month. Those peaks can be indexed to the (111), (200), (220), and (311) diffractions of the standard face-centered-cubic phase metallic Ag 447 (JCPDS No. 04-0783). No characteristic diffraction peaks were found for AgO, indicating chemical stability.

Mechanical and thermal properties

The mechanical properties of cotton fibers were investigated in consideration of possible damages caused by high temperature and potential chemical interactions among cotton, HBPAA, and HBPAE. Pure cotton fibers showed an average tensile stress of 2.31 cN/dtex and an average strain to failure of 7.93% (Table 1). The tensile stress of AgNP-coated cotton fibers slightly decreased, whereas their strain to failure marginally increased, indicating that assembly may slightly reduce the crystallinity of cotton fibers. Compared with pure cotton, the tensile modulus decreased for 3 mg/g of AgNP-coated cotton fibers but slightly increased for 15 mg/g of coated fibers. Cotton fibers became harder when the cotton surface was coated by dense AgNPs. In summary, the coated cotton fibers retained their original mechanical properties after treatment.

Figure 9 shows the thermogravimetric curves of pure cotton fibers and 3 and 15 mg/g of heterostructured AgNP-coated cotton fibers. Pure cotton fibers possessed good thermal stability until temperature reached 270 °C and then were decomposed into aliphatic char and volatile products when temperature increased from 270 to 381 °C. The conversion of aliphatic char into aromatic, generating carbon mono and dioxide, occurred at approximately 483 °C (Alongi et al. 2012). For heterostructured AgNP-coated cotton fibers, considering that AgNPs, HBPAA,

Table 1 Mechanical properties of cotton fibers and heterostructured AgNP-coated cotton fibers

Samples	Ag content (mg/g)	Tensile stress (cN/dtex)	Strain to failure (%)	Tensile modulus (cN/dtex)
Cotton fibers	0	2.31 ± 0.65	7.93 ± 2.93	30.23 ± 4.78
AgNP-coated cotton fibers	3	2.15 ± 0.44	8.52 ± 1.9	27.47 ± 6.61
	15	2.12 ± 0.64	8.84 ± 3.89	30.81 ± 8.69

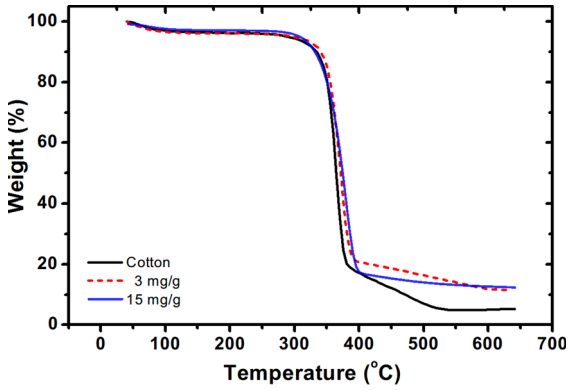

Fig. 9 Thermogravimetric curves of pure cotton fibers (*black*) and 3 (*red*) and 15 mg/g (*blue*) of heterostructured AgNP-coated cotton fibers. (Color figure online)

and HBPAE showed better thermal stability than cotton, heterostructured AgNPs could act as a physical barrier, which can isolate cotton from heat and oxygen. Both 3 and 15 mg/g of heterostructured AgNP-coated cotton fibers showed slightly higher decomposition temperature and less weight loss even after 600 °C than pure cotton fibers (Fig. 9). The coating of heterostructured AgNPs could slightly improve the thermal stability of cotton fibers (Ravindra et al. 2010).

Antimicrobial activity of the heterostructured AgNP-coated cotton fibers

The heterostructured AgNP-coated cotton fibers with Ag content from 1.5 to 15 mg/g were fabricated by the method described above, and their antibacterial activities against *E. coli* and *S. aureus* were quantitatively measured using the shake-flask method. Compared with pure cotton fibers, the heterostructured AgNP-coated cotton fibers exhibited excellent antibacterial activities against *E. coli* and *S. aureus* (Table 2). The inhibition rates of *E. coli* and *S. aureus* both exceeded 99% when the Ag content was only 1.5 mg/g. As expected, the heterostructured AgNP-coated cotton fibers also showed Ag-content-dependent antimicrobial activity. The antibacterial rates against *E. coli* and *S. aureus* increased from 99.93 and 98.93% to 99.95 and 99.91%, respectively, as Ag content increased from 1.5 to 3 mg/g. With further increase in Ag content to 6 and 15 mg/g, almost all of the *E. coli* and *S. aureus* were killed, indicating the materials' powerful antibacterial effects. Notably, the antibacterial function of the coated cotton was derived from the synergistic effects of the AgNPs and the capping molecules. The functionalization of NP surfaces with HBPAA and HBPAE endowed the NPs with molecular selectivity, affecting their surface binding to bacterial cells. Particularly, the HBPAA and HBPAE molecules on the AgNP surfaces can trap lipopolysaccharide- and peptidoglycan-containing *E. coli* and *S. aureus* onto the cotton fiber surface by electrostatic or hydrogen-bonding interactions because of their highly active amino and hydroxyl groups. Consequently, the NPs exhibited efficient antibacterial activities.

Conclusions

Heterostructured AgNP-coated cotton fibers with tunable Ag content were fabricated by an eco-friendly approach through supramolecular cooperative self-assembly of mutually recognized HBPAA/AgNPs and HBPAA/AgNPs. The as-synthesized HBPAA/AgNPs and HBPAE/AgNPs possessed opposite charges and high density of amino and hydroxyl groups,

Table 2 Ag-content-dependent antibacterial activities of cotton fibers against *E. coli* and *S. aureus*

Cotton samples	Ag content (mg/g)	Antibacterial activities			
		E. coli		*S. aureus*	
		Surviving cells (cfu/mL)	% Reduction	Surviving cells (cfu/mL)	% Reduction
Cotton fibers	–	4.52×10^6	–	1.37×10^7	–
	1.5	1.89×10^2	99.93	3.64×10^3	98.93
	3	1.35×10^2	99.95	3.06×10^2	99.91
Coated cotton fibers	4.5	56	99.98	1.36×10^2	99.96
	6	31	99.99	37	99.99
	15	0	100	0	100

respectively, which were capable of forming strong electrostatic and intermolecular hydrogen-bonding interactions. The generation of a special heterostructured coating was dependent on two important characteristics. One is the good binding affinity of the HBPAA/AgNPs toward cotton cellulose derived from their dense functional amino groups. This attribute rendered the initial self-assembly between the HBPAA/AgNPs and cotton fibers possible. The other attribute is the ability of the HBPAA/AgNPs and HBPAE/AgNPs to mutually recognize and combine through ultra-strong supramolecular interactions. Therefore, the two distinct AgNPs could cooperatively self-assemble onto the cotton surface through a well-designed step-by-step assembly process. Specifically, heterostructured AgNP-coated cotton fibers were fabricated by the circular incubation of cotton fibers with HBPAA/AgNPs and HBPAE/AgNPs at room temperature. By carefully controlling the AgNP concentration and incubation time, the complete adsorption of heterostructured AgNPs on cotton fibers could be achieved. Further studies showed that the cooperative self-assembly maintained their high efficiency even after five cycle treatments. FESEM measurement suggested that the constructed heterostructured AgNP coating showed good uniformity, although a fraction of Ag nanoclusters exited. XPS and XRD analyses demonstrated the good chemical stability of AgNPs after spatial transfer from water to the organic solid surface, probably owing to the excellent protection afforded by HBPAA and HBPAE. Further researches showed that the mechanical and thermal properties of cotton fibers have no obvious changes after the treatment. The antibacterial tests showed that the fabricated heterostructured AgNP-coated cotton fibers exhibited Ag-content-dependent and tunable antibacterial ability because the Ag content in the cotton fibers could be precisely controlled. In summary, the advantages of cooperative self-assembly technology include environmental friendliness, precise control of Ag content, and high self-assembly capacity, indicating their potential application in antibacterial textiles.

Acknowledgment The authors acknowledge the financial support of JSPS KAKENHI (Japan) (No. 15H01789), the Science and Technology Support Program of Jiangsu Provincial Department (China) (No. BE2013649), the Jiangsu Qing Lan Project (China), and the Prospective Industry-Academic Cooperation Project of Jiangsu Province (China) (No. BY2016053-13).

References

Abidi N, Hequet E, Cabrales L, Gannaway J, Wilkins T, Wells LW (2008) Evaluating cell wall structure and composition of developing cotton fibers using Fourier transform infrared spectroscopy and thermogravimetric analysis. J Appl Polym Sci 107:476–486. doi:10.1002/app.27100

Alongi J, Ciobanu M, Malucelli G (2012) Thermal stability, flame retardancy and mechanical properties of cotton fabrics treated with inorganic coatings synthesized through sol–gel processes. Carbohydr Polym 87:2093–2099. doi:10.1016/j.carbpol.2011.10.032

Bao L, Li X (2012) Towards textile energy storage from cotton T-shirts. Adv Mater 24:3246–3252. doi:10.1002/adma.201200246

Eckhardt S, Brunetto PS, Gagnon J, Priebe M, Giese B, Fromm KM (2013) Nanobio silver: its interactions with peptides and bacteria, and its uses in medicine. Chem Rev 113:4708–4754. doi:10.1021/cr300288v

French AD (2014) Idealized powder diffraction patterns for cellulose polymorphs. Cellulose 21:885–896. doi:10.1007/s10570-013-0030-4

Grzelczak M, Vermant J, Furst EM, Liz-Marzán LM (2010) Directed self-assembly of nanoparticles. ACS Nano 4:3591–3605. doi:10.1021/nn100869j

Hsu P-C et al (2015) Personal thermal management by metallic nanowire-coated textile. Nano Lett 15:365–371. doi:10.1021/nl5036572

Huda S, Smoukov SK, Nakanishi H, Kowalczyk B, Bishop K, Grzybowski BA (2010) Antibacterial nanoparticle monolayers prepared on chemically inert surfaces by cooperative electrostatic adsorption (CELA). ACS Appl Mater Interfaces 2:1206–1210. doi:10.1021/am100045v

Kaegi R et al (2013) Fate and transformation of silver nanoparticles in urban wastewater systems. Water Res 47:3866–3877. doi:10.1016/j.watres.2012.11.060

Khan Y, Ostfeld AE, Lochner CM, Pierre A, Arias AC (2016) Monitoring of vital signs with flexible and wearable medical devices. Adv Mater. doi:10.1002/adma.201504366

Kuzyk A et al. (2012) DNA-based self-assembly of chiral plasmonic nanostructures with tailored optical response. Nature 483:311–314 doi:http://www.nature.com/nature/journal/v483/n7389/abs/nature10889.html#supplementary-information

Lee I, Evans BR, Woodward J (2000) The mechanism of cellulase action on cotton fibers: evidence from atomic force microscopy. Ultramicroscopy 82:213–221. doi:10.1016/S0304-3991(99)00158-8

Levard C, Hotze EM, Lowry GV, Brown GE (2012) Environmental transformations of silver nanoparticles: impact on stability and toxicity. Environ Sci Technol 46:6900–6914. doi:10.1021/es2037405

Li Y, Liu Z, Yu G, Jiang W, Mao C (2015) Self-assembly of molecule-like nanoparticle clusters directed by DNA nanocages. J Am Chem Soc 137:4320–4323. doi:10.1021/jacs.5b01196

Liu N et al (2013) Cable-type supercapacitors of three-dimensional cotton thread based multi-grade nanostructures for wearable energy storage. Adv Mater 25:4925–4931. doi:10.1002/adma.201301311

Lu Y, Sathasivam S, Song J, Crick CR, Carmalt CJ, Parkin IP (2015) Repellent materials Robust self-cleaning surfaces that function when exposed to either air or oil. Science 347:1132–1135. doi:10.1126/science.aaa0946

Nykypanchuk D, Maye MM, van der Lelie D, Gang O (2008) DNA-guided crystallization of colloidal nanoparticles. Nature 451:549–552 doi:http://www.nature.com/nature/journal/v451/n7178/suppinfo/nature06560_S1.html

Peng S, Gao Z, Sun J, Yao L, Qiu Y (2009) Influence of argon/oxygen atmospheric dielectric barrier discharge treatment on desizing and scouring of poly (vinyl alcohol) on cotton fabrics. Appl Surf Sci 255:9458–9462. doi:10.1016/j.apsusc.2009.07.058

Rai M, Yadav A, Gade A (2009) Silver nanoparticles as a new generation of antimicrobials. Biotechnol Adv 27:76–83. doi:10.1016/j.biotechadv.2008.09.002

Ravindra S, Murali Mohan Y, Narayana Reddy N, Mohana Raju K (2010) Fabrication of antibacterial cotton fibres loaded with silver nanoparticles via "Green Approach". Colloids Surf A Physicochem Eng Asp 367:31–40. doi:10.1016/j.colsurfa.2010.06.013

Richter AP et al. (2015) An environmentally benign antimicrobial nanoparticle based on a silver-infused lignin core. Nat Nano 10:817–823 doi:10.1038/nnano.2015.141. http://www.nature.com/nnano/journal/v10/n9/abs/nnano.2015.141.html#supplementary-information

Rogers WB, Shih WM, Manoharan VN (2016) Using DNA to program the self-assembly of colloidal nanoparticles and microparticles. Nat Rev Mater 1:16008. doi:10.1038/natrevmats.2016.8

Roopan SM, Rohit Madhumitha G, Rahuman AA, Kamaraj C, Bharathi A, Surendra TV (2013) Low-cost and eco-friendly phyto-synthesis of silver nanoparticles using Cocos nucifera coir extract and its larvicidal activity. Ind Crops Prod 43:631–635. doi:10.1016/j.indcrop.2012.08.013

Schoen DT, Schoen AP, Hu L, Kim HS, Heilshorn SC, Cui Y (2010) High speed water sterilization using one-dimensional nanostructures. Nano Lett 10:3628–3632. doi:10.1021/nl101944e

Xu S, Zhang F, Song J, Kishimoto Y, Morikawa H (2015) Preparation of silver nanoparticle-coated calcium alginate fibers by hyperbranched poly(amidoamine)-mediated assembly and their antibacterial activity. Text Res J. doi:10.1177/0040517515599745

Xu S et al (2016a) Preparation and controlled coating of hydroxyl-modified silver nanoparticles on silk fibers through intermolecular interaction-induced self-assembly. Mater Des 95:107–118. doi:10.1016/j.matdes.2016.01.104

Xu S, Zhang F, Song J, Kishimoto Y, Morikawa H (2016b) Preparation of silver nanoparticle-coated calcium alginate fibers by hyperbranched poly(amidoamine)-mediated assembly and their antibacterial activity. Text Res J 86:878–886. doi:10.1177/0040517515599745

Yu S-J, Yin Y-G, Liu J-F (2013) Silver nanoparticles in the environment. Environ Sci Process Impacts 15:78–92. doi:10.1039/C2EM30595J

Zeng W, Shu L, Li Q, Chen S, Wang F, Tao X-M (2014) Fiber-based wearable electronics: a review of materials fabrication, devices, and applications. Adv Mater 26:5310–5336. doi:10.1002/adma.201400633

Zhang Y, Lu F, Yager KG, van der Lelie D, Gang O (2013) A general strategy for the DNA-mediated self-assembly of functional nanoparticles into heterogeneous systems. Nat Nano 8:865–872 doi:10.1038/nnano.2013.209. http://www.nature.com/nnano/journal/v8/n11/abs/nnano.2013.209.html#supplementary-information